frontiers | Frontiers in Physics

TYPE Mini Review
PUBLISHED 20 December 2022
DOI 10.3389/fphy.2022.1102996

OPEN ACCESS

EDITED BY
Tonglei Cheng,
Northeastern University, China

REVIEWED BY
Lee Xiaobao,
Hunan University of Technology, China
Xuebin Sun,
Tianjin University, China
Yang Qu,
Nanjing Vocational College of Information Technology, China

*CORRESPONDENCE
Yajun Pang,
yjpang@hebut.edu.cn

SPECIALTY SECTION
This article was submitted to Optics and Photonics, a section of the journal
Frontiers in Physics

RECEIVED 19 November 2022
ACCEPTED 05 December 2022
PUBLISHED 20 December 2022

CITATION
Pang Y, Zhang K and Lang L (2022), Review of acousto-optic spectral systems and applications.
Front. Phys. 10:1102996.
doi: 10.3389/fphy.2022.1102996

Review of acousto-optic spectral systems and applications

Yajun Pang[1,2]*, Kai Zhang[1,2] and Liying Lang[1,2]

[1]Center for Advanced Laser Technology, Hebei University of Technology, Tianjin, China, [2]Hebei Key Laboratory of Advanced Laser Technology and Equipment, Tianjin, China

Acousto-optic devices represented by acousto-optic tunable filters (AOTFs), have the advantages of wide wavelength range from the ultraviolet to the long-wave infrared and fast wavelength switching speed. Nowadays, acousto-optic spectral systems have become very important scientific instruments in laboratory. There are many factors to be considered when we choose different solutions for acousto-optic spectral systems, but there is no comprehensive analysis and summary of them. This paper explains the working principle of the acousto-optic devices and summarizes the most common optical schemes for acousto-optic spectral systems. We also analyzed their characteristics of application conditions. In addition, specific applications of acousto-optic spectral systems in some common fields are presented.

KEYWORDS

spectral devices, imaging spectrometer, acousto-optic tunable filter (AOTF), optical schemes, acousto-optic effect

1 Introduction

The study of acousto-optic interactions began in the 1920s and was limited to isotropic media such as water and glass [1, 2]. When ultrasonic waves pass through the medium, the refractive index of the medium changes periodically by the modulation of the strain. The acousto-optic medium is equivalent to a dislocation grating, and diffraction occurs when light passes through it. With the emergence of lasers and high-performance acousto-optic crystals, the study of acousto-optic devices has broadened from isotropic to anisotropic media and from normal to anomalous interactions [3–5]. As the research of acousto-optic theory continues to progress, the principles of isotropic and anisotropic acousto-optic interactions need to be unified. We can consider the acousto-optic effect as a parametric interaction process, which is described by the relationship between the non-linear polarization vector and the strain [6–8].

The first AOTF was proposed by Harris and Wallace utilizing the collinear acousto-optic interaction [9]. In 1974, I. C. Chang proposed the idea of a non-collinear acousto-optic tunable filter design, which laid a solid foundation for the development of acousto-optic devices [10]. When an excitation RF signal of a certain frequency is applied to the transducer, the piezoelectric crystal transducer converts it into an ultrasonic signal of the corresponding frequency and couples it into the birefringent crystal. The refractive index of the crystal then changes periodically, which is equivalent to the formation of a bit-phase grating in the crystal, and the grating constant is the wavelength of ultrasonic waves

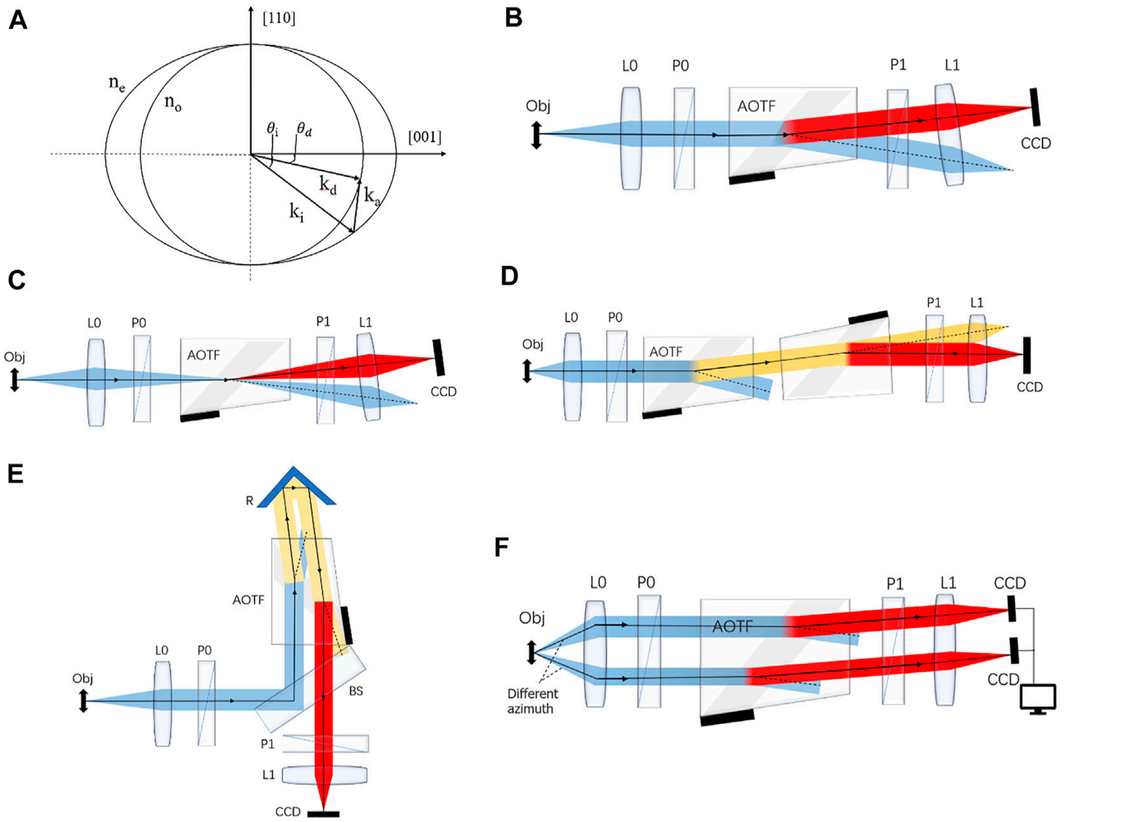

FIGURE 1
(A) Non-collinear acousto-optic interaction wave vector diagram in TeO_2, **(B)** collimating scheme, **(C)** confocal scheme, **(D)** tandem scheme, **(E)** double-pass single-crystal AOTF based spectral scheme, **(F)** double-path scheme (Obj, object; L, lens; P, polarizer; R, retroreflector; BS, beam splitter; CCD, charge-coupled device).

[11–14]. The acousto-optic interaction wave vector diagram, which takes place in AOTF, is shown in Figure 1A. The incident light wave vector $\mathbf{k_i}$, diffracted light wave vector $\mathbf{k_d}$, and the acoustic wave vector $\mathbf{k_a}$ are strictly matched to the momentum triangle closure condition:

$$\overrightarrow{k_d} = \overrightarrow{k_a} \pm \overrightarrow{k_i} \tag{1}$$

$$k_i = \frac{2\pi n_i}{\lambda}, k_d = \frac{2\pi n_d}{\lambda}, k_a = \frac{2\pi f_a}{v_a} \tag{2}$$

Where n_i is the refractive index of the crystal to the incident light, and n_d is the refractive index of the crystal to the diffracted light. The incident angle θ_i and diffraction angle θ_d are shown in Figure 1A. λ is the optical wavelength in vacuum, f_a is the acoustic frequency, and v_a is the speed of the ultrasonic wave.

In the case of collinear acousto-optic interaction, the incident light wave vector, the diffracted light wave vector and the ultrasonic wave vector are in the same direction. The momentum matching triangle at this point is simplified to a straight line. The geometric relationship between the vectors can be turned into an algebraic sum. Bringing Eq. 2 into Eq. 1, the tuning equation of the common-linear acousto-optic tunable filter can be obtained as

$$\lambda f_a = \pm v_a (n_d - n_i) \tag{3}$$

In the non-collinear case, the diffracted light and the incident light propagate in different intrinsic modes in the crystal, and the incident light wave vector and the diffracted light wave vector are not parallel. The incident light wave vector, the ultrasonic wave vector and the diffracted light wave vector are in a vector triangle relationship (i.e., momentum matching condition). Usually, in the design of AOTF, the tangents of the incident and diffracted light wavevectors are parallel to each other at the corresponding wavevector surface in order to have a large incident angle aperture. In this case, the design parameters are related as follows

$$n_i = \left[\frac{\cos^2\theta_i}{n_o^2} + \frac{\sin^2\theta_i}{n_e^2}\right]^{-1/2} \tag{4}$$

$$n_d = n_o \tag{5}$$

n_o and n_e are the refractive indices of ordinary ray and extraordinary ray which are perpendicular to the optical axis, and they are a function of the wavelength of light. According to the tangential parallelism condition, the relationship between the diffracted light polar angle and the incident light polar angle is

$$\tan\theta_d = (n_o/n_e)^2 \quad (6)$$

The tuning relationship between optical wavelength and ultrasonic frequency can be expressed by

$$f_a = \frac{v_a}{\lambda}\left(n_i^2 + n_d^2 - 2n_i n_d \cos(\theta_i - \theta_d)\right)^{\frac{1}{2}} \quad (7)$$

Combining Eqs 1–3, we can simplify Eq. 4 to

$$f_a = \frac{v_a}{\lambda}(n_i - n_d)\left(\sin^2 2\theta_i + \sin^4\theta_i\right)^{\frac{1}{2}} \quad (8)$$

Exceptionally, when $\theta_i = 90°$, the equation reduces to the tuning relationship for the common-linear interaction. Therefore, the collinear interaction can be viewed as a special case of non-collinear interaction. The non-collinear AOTF keeps the tangents of the incident light and the diffracted light on the wave vector trajectory parallel to each other, so that when there is a small change for the incident angle, the momentum matching condition still holds.

There are many applications based on acousto-optic action, such as acousto-optic modulators, deflectors, frequency shifters, and tunable filters. The AOTFs are becoming a widely used tool for these applications. Spectral imagers based on AOTF have a wide range of applications in science and engineering [15–17]. Although there have been many reports on the generation and application of AOTF acousto-optic spectral instruments, there is no comprehensive summary of the characteristics of different schemes. In this paper, we summarize in detail the commonly used optical schemes for AOTF-based acousto-optic spectral systems and compare them with examples, and finally present specific applications in major representative fields.

2 Acousto-optic spectral system schemes

AOTFs have a variety of applications, and researchers have used a variety of different optical solutions for purposes [18, 19]. Different schemes differ in image quality, the number of coupling components, size, and alignment complexity [20–22]. To properly select the optical system for an AOTF-based spectral system, many factors must be considered [23–25]. Although various acousto-optic filtering schemes have been tested and discussed in various articles, a summary of them is not available so far. In this section, the four most common optical schemes based on the AOTF module as shown in Figure 1 are presented: collimating scheme, confocal scheme, tandem scheme, and double-path scheme. We will compare and analyze their main features with some examples. Although these schemes are derived from both collimation and confocal schemes, this division makes them easier to be summarized as well as to be understood.

2.1 Collimating scheme

For conventional acousto-optic spectral systems, the collimating scheme is the most common and structurally simple scheme, and the optical path diagram is shown in Figure 1B. The adopted scheme is to filter the light directly using a single AOTF, which is also the basis of other schemes [26, 27]. The light entering the optical system from the object under test is collimated by L0, the mutually parallel light is filtered by the AOTF, and then be focused on the CCD by the focusing lens L1. Non-uniformity of the central wavelength of the filtered light across the field of view can lead to specific image spectral distortions [28].

The conventional acousto-optic spectral system can satisfy the needs of many tasks. But, the optimization of this system is necessary, and the integration of the optimized AOTF units into other schemes can multiply the efficiency. In 2021, proposed a method for optimizing the size of piezoelectric transducers of quasi-collinear AOTF [29]. In this scheme, they used an AOTF with a large interaction length. From the experimental results, it is shown that the variation of the transducer size can minimize the RF power consumption of the AOTF. Comparing the optimized transducer dimensions with those commonly used ones in quasi-collinear AOTF, the optimized AOTF energy efficiency can be improved about twice.

2.2 Confocal scheme

Confocal optics can compensate for almost any degree of AOTF diffraction aberration. Unlike wedge compensation, this optical system does not require dispersion and can be used with any type of AOTF [30–32]. The confocal optics scheme is shown in Figure 1C. The use of telecentric confocal optics can eliminate errors caused by inaccurate focus. In addition, the system has the advantage of uniform image field with the same resolution and diffraction efficiency over the scene [33, 34]. However, the focal length of the lens in the system must be shot enough to prevent diffraction from limiting resolution.

In 2019, combined AOTF with a rigid borescope, a flexible fiberscope, and a video endoscope, and designed an acousto-optic spectral imaging endoscopic analysis system for observing cancerous tissue [35]. This scheme uses a confocal optical design that can provide high-quality spectral images. This solution can be very effective in solving different specific tasks in biomedical and industrial fields. The main aberration in the confocal scheme is from the presence of longitudinal color focus shift and lateral chromatic image drift. However, this color difference can be almost completely compensated by adjusting the tilt of the output side of the acousto-optic unit to the input side. While, in the collimating scheme, the main aberration is the transverse chromatic aberration, which can be eliminated by choosing a different tilt angle [36, 37].

Collimating and confocal optical schemes both have their own advantages and disadvantages, the confocal scheme is not the optimization of the collimated scheme. In 2021, a super-angular aperture scheme was proposed by [38]. They used both schemes to quantify the change in radiation flux caused by the super-angular aperture scheme and the response of the AOTF element at tilted incidence. They analyzed the system response of the collimated and confocal optical schemes and verified the simulation results. The collimated optical path was found to be more suitable for the super-angular aperture scheme by comparing the two optical schemes. This is because its spectral bandwidth is better than that of the confocal optical scheme, and the central wavelength shift can be corrected by calibration.

2.3 Tandem scheme

The most common and straightforward application of the double filter structure is to connect two AOTFs in series. In 2018, Lei Shi et al. designed a series of double filtering schemes [39]. They compared the spectral widths at different frequencies by analyzing the experimental data. It was finally found that the double-filter structure reduced the spectral width by an average of 37% and improved the spectral resolution by an average of 57% compared to the single filter. By analyzing and comparing the theoretical calculations and experimental measurements of the properties of single and double filter structures, we can find that the spectral width of the double filter structure is smaller than that of the single filter structure for equal central wavelengths. This situation illustrates the superiority of the double-filter technique in improving the spectral width and in increasing the spectral resolution [40].

In 2019, Vitoid E. Pozhar et al. designed a system architecture to address the problem of creating hyperspectral optoelectronic systems for unmanned aerial vehicles [41]. The developed hyperspectrometer uses a dual compact AO monochromator as a spectral element. It consists of two identical AO cells, deployed by 180°, which provides compensation for most spatial spectral aberrations. The device's small size, low power consumption, and ability to obtain both spectral and color images with high spectral (~5 nm) and spatial (600–500 elements) resolution over a sufficiently wide wavelength range (450–850) nm make it possible to use it effectively on unmanned aerial vehicles. In fact, back in 2005, Pozhar and other researchers proposed a double-AOTF spectral imaging system for microscopic analysis in the visible and near-infrared range, and it was shown that double AOTF monochromator ensures improved image quality than single imaging AOTF [42].

Tandem AOTF is only one way to realize double filtering, in addition, there are different ways such as the single-crystal double filtering technique. The optical scheme design diagram is shown in Figure 1D. Double filtering is realized using a single crystal, but structurally it is similar to double filtering using two AOTFs. It is simpler and more economical to realize double filtering using a single crystal. Therefore, the scheme of the series connection is less used in practical applications, and nowadays, the single crystal double filtering technique is more often used.

In 2019, Xiaofa Zhang et al. designed a single-crystal double filtering hyperspectral microscopic imaging system [43]. By analyzing the experimental results of diffracted light spectrograms of single-crystal double-filtering scheme, we can find that the comparison yielded a double-filter structure with an average 32% reduction in spectral width compared to single-filtering at a fixed ultrasound frequency of 120 MHz. In the visible range, the spectral resolution can be improved by 37.08%–59.95%. In addition, in 2021, Vladislav Batshev et al. similarly devised a method to improve the spectral resolution of a single AOTF by using a single-crystal for secondary filtering [44]. The structure is similar to Figure 1E. From the results, the transmission spectral width at the 0.5 level (FWHM) is about 1.3 times smaller than that of the classical single-pass scheme.

Among the three schemes mentioned above, the series double-filtering system designed by Shi Lei et al. works best from the results. But unfortunately, the specific series filtering method does not appear in the article. The double-filtering technique can effectively improve the spectral resolution of the acousto-optic filters. In addition, the primary filtered signal after the AOTF is accompanied by an obvious side flap phenomenon, which comes from the acousto-optic interaction [45–48]. There is no way to eliminate the side flaps by using the primary filtering technique. After double-pass filtering, the side flaps are suppressed very significantly, which can improve the spectral purity of the diffracted light [49].

2.4 Double-path scheme

For double-path acousto-optic spectroscopy systems or multi-path analysis systems, they are often used in special scenarios to meet specific requirements [50, 51].

Khoptyar et al. published two articles back and forth in 2012 and 2013 on the use of double-path optical schemes to fabricate novel photon time-of-flight spectrometers for the analysis of turbid media [52, 53]. The wide spectral range of the instrument helps to characterize the structure of the sample and to obtain excellent accuracy in the measurement of absorption and scattering coefficients. Photon time-of-flight spectrometers are used for the evaluation of pharmaceutical chemical composition analysis with proven results. Therefore,

TABLE 1 Comparison of acousto-optic spectral analysis system schemes.

Type	Advantages	Disadvantages	Spectral range/nm	Angular aperture/°	Spectral band/nm	Ref
Collimating scheme	1. The structure is simple and easy to build	1. Non-uniformity of the central wavelength of the filtered light across the field of view can lead to specific image spectral distortions	700–1,150	0.04	0.3@633	[27]
	2. It is stable and can be used as a component in various systems	2. The scheme has transverse chromatic aberration				
Confocal scheme	1. The structure is simple and easy to build	1. The presence of longitudinal color focus shift and lateral chromatic image drift produce aberration	450–750	—	4.5@632	[33]
	2. Compensate for almost any degree of AOTF diffraction aberration					
Tandem scheme	1. It can reduce the spectrum width and improve the spectral resolution	1. Diffraction efficiency will be reduced	400–1,000	2.83	2.9@632.5	[37]
	2. The scheme can effectively lower the side flaps		400–1,000	3	3.44@651.62	[39]
			450–850	4	3@600	[40]
Double-path scheme	1. The structure can obtain more complete and richer spectral information	1. Specific solutions in different applications need to be designed	450–850	—	~3@625	[50]
	2. The design of the structures in different practical applications will be flexible					

10.3389/fphy.2022.1102996

double-path optical systems and triple-path spectral systems tend to demand high precision as well as wide spectrum.

In 2019, Ramy Abdlaty and Qiyin Fang both designed an AOTF-based hyperspectral imaging system [54]. Object illumination is provided from both sides to provide uniformly distributed illumination and to avoid shadowing problems. The light reflected from the object is captured by the zoom lens and beam shaping optics. Polarization beam splitter (PBS) splits the collimated beam into two orthogonally polarized beams of transmitted and reflected light. The polarization of the PBS reflected beam is rotated using a half-wave plate to match the PBS transmitted beam. The two PBS beams have the same polarization matched to the AOTF crystal, and this polarization matching allows them to come to the maximum diffraction efficiency.

In 2020, Alexander Machikhin et al. proposed a new concept of spectral stereo imaging [55]. The stereo imaging optical system is shown in Figure 1F. This stereo imaging system is based on simultaneous wide-aperture acousto-optic diffraction of two beams through a conventional AOTF. Experimental results have shown that the quality of the spectral images is quite high, which is necessary for the stereo reconstruction process. In 2021, A. A. Naumov proposed an optical stereo system [56], and this system is very similar to the structure of Figure 1E. The characteristics of such optical systems depend to a large extent on three parameters: the focal length of the incident lens, the focal length of the matrix sensor lens, and the diameter of the incident optical pupil of the acousto-optic filter. The variability of these parameters allows the optical system to be adapted to different tasks [57].

The photon time-of-flight spectrometer utilizes an AOTF module with only partial overlap of the two spectral bands, and the results of the two spectral bands are stitched together to obtain broad-spectrum information. In contrast, in the hyperspectral imaging system, the information of both line polarized beams is processed and retained to obtain the complete spectrum. The two cases of stereo imaging have the same principle, both of which collect the spectral information observed in different orientations and then reorganize them. From the previous analysis, it can be known that both double-path acousto-optic spectral analysis systems aim to obtain more complete spectral information, only the way and results are different. The double-path scheme allows for a wider spectral range than other optical schemes as well as a more complete spectral information from different angles of the same object. At the same time, the flexible placement of the device may also bring more possibilities for spectral system detection. The double pathway acousto-optic spectroscopy system has been used in practical devices for stereoscopic imaging, drug characterization, and multi-directional evaluation after continuous experimentation and is still being improved.

Each scheme have different features and resolutions, the comparison is shown in Table 1.

3 Applications

Acousto-optic devices are used more frequently in representative fields such as medical and healthcare, aerospace, and food safety. Due to the small mass, small size, absence of removable elements, and compact construction of the AOTF, acousto-optic filters are ideally suited for use with devices used to view hard-to-reach objects, such as rigid lenses and flexible fiberoptic endoscopes [58–61]. The application of acousto-endoscopic imaging spectroscopy will significantly reduce the cost of laboratory testing and increase the information density of research [62–64]. In addition, the development of space instruments based on AOTFs has enhanced the detection capabilities of various space probes. In 2019, He et al. summarized the acousto-optic spectrometers used by China in recent years for lunar exploration [65]. The study include the infrared imaging spectrometer on Chang'e 3 and Chang'e 4 lunar rovers, and the lunar mineral spectrometry analyzer on the Chang'e 5 and Chang'e 6 lunar landers. Acousto-optic devices are becoming widely used in planetary observation, laser observation, surface positioning, and remote sensing [66–69].

Acousto-optic hyperspectral imaging detection technology has also been applied to the detection of microorganisms. In 2018, Y. Seo et al. used acousto-optic spectral image processing techniques for extracting information related to morphological characteristics of 15 different foodborne bacterial species and serotypes [70]. This study achieved a cost-effective classification of foodborne bacteria. In addition, acousto-optic spectroscopy detection systems are also used to test meat, grains and even liquid foods [71–77]. For example, in 2021, I. Baek et al. proposed a short-wave infrared hyperspectral imaging system for the detection of total volatile basic nitrogen content in fresh pork. This system can be used for rapid non-destructive assessment of pork freshness and can be an effective alternative to traditional methods for assessing pork freshness [78].

In addition, acousto-optic spectroscopy systems are also widely used in agriculture, forestry, pharmaceutical analysis, and environmental monitoring [79]. Hong Liu et al. designed a drone-based hyperspectral imaging remote sensing system in 2021 [80], which can be used for activities such as water surface remote sensing, imaging, and spectral analysis. In agriculture, a commercial AOTF-based near-infrared spectrometer is already available for the non-destructive detection of agricultural products such as dried apples and olive fruit [81]. Acousto-optic spectroscopy systems are becoming more and more relevant to our lives.

With the development of various new technologies, the miniaturization and intelligence of spectrometers equipped with acousto-optic spectral analysis systems are becoming more obvious. Like the applications of acousto-optic spectral analysis instruments in various fields described above, acousto-optic devices are now used in a large number of fields. The application of acousto-optic spectral systems is likely to be associated with the development of new materials and new energy sources in the future. Not only for the test of new materials, but also for improving the performance of acousto-optic spectral systems in combination with new materials. The acousto-optic spectral analysis systems are expected to get more long-term development.

4 Conclusion

This article focuses on review of the basic construction of four different optical schemes based on AOTF. Due to the simplicity of the acousto-optic spectral systems, these four optical schemes can be easily embedded in different application scenarios. We summarize the advantages and disadvantages of the different schemes by analyzing the characteristics of the four optical schemes. At the same time, we compare the different schemes with each other and provide theoretical references for the application in different scenarios. Acousto-optic spectral systems have great potential for development in various fields, but in order to adapt to different application scenarios, the requirements for each parameter of the acousto-optic device become higher. The relevant summary and the analysis of characteristics described are expected to provide references for further applications of acousto-optic spectral technology.

Author contributions

YP: Investigation, writing—original draft, writing—review and editing, supervision. KZ: Investigation, writing—original draft. LL: Investigation, writing—review and editing.

Funding

This work was supported by the National Natural Science Foundation of China (61905063), Natural Science Foundation of Hebei Province (F2020202055).

Conflict of interest

The authors declare that the research was conducted in the absence of any commercial or financial relationships that could be construed as a potential conflict of interest.

Publisher's note

All claims expressed in this article are solely those of the authors and do not necessarily represent those of their affiliated organizations, or those of the publisher, the editors and the reviewers. Any product that may be evaluated in this article, or claim that may be made by its manufacturer, is not guaranteed or endorsed by the publisher.

References

1. Chang I. Acousto-optic tunable filters. *Opt Eng* (1981) 20(6):206824. doi:10.1117/12.7972821

2. Brillouin L. Diffusion de la lumière et des rayons X par un corps transparent homogène. *Ann Phys* (1922) 17(2):88–122. doi:10.1051/anphys/192209170088

3. Cheong Y., Popa B-I. Acousto-optical metasurfaces for high-resolution acoustic imaging systems. *Phys Rev B* (2021) 104(14):L140304. doi:10.1103/physrevb.104.l140304

4. Goutzoulis AP. *Design and fabrication of acousto-optic devices*. Boca Raton: CRC Press (2021).

5. V Pozhar A Machikhin, editors. Acousto-optical imaging spectroscopy. In: 2021 Wave Electronics and its Application in Information and Telecommunication Systems (WECONF). IEEE (2021).

6. S Mantsevich, V Balakshy, Y Kuznetsov, editors. Acousto-optic spectrum analyzer-the new type of optoelectronic device. In: International Conference on Photonics, Optics and Laser Technology, Porto, February 27–March 1, 2017 (Porto: SCITEPRESS) (2017).

7. Balakshy VI. Acousto-optic visualization of optical wavefronts [Invited]. *Appl Opt* (2018) 57(10):C56–C63. doi:10.1364/ao.57.000c56

8. Bader T. Acoustooptic spectrum analysis: A high performance hybrid technique. *Appl Opt* (1979) 18(10):1668–72. doi:10.1364/ao.18.001668

9. Harris S, Wallace R. Acousto-optic tunable filter. *J Opt Soc Am* (1969) 59(6):744–7. doi:10.1364/josa.59.000744

10. chang IC. Noncollinear acousto-optic filter with large angular aperture. *Appl Phys Lett* (1974) 25(7):370–2. doi:10.1063/1.1655512

11. Machihin A, Pozhar V. Spatial and spectral image distortions caused by diffraction of an ordinary polarised light beam by an ultrasonic wave. *Quan Elec (Woodbury)* (2015) 45(2):161–5. doi:10.1070/qe2015v045n02abeh015385

12. S Mantsevich, V Balakshy, editors. The peculiarities of collinear acousto-optic filtration in the presence of optoelectronic feedback. In: 2018 4th International Conference on Frontiers of Signal Processing (ICFSP), Poitiers, France, September 24-27, 2018. (Poitiers, France: IEEE) (2018).

13. Voloshinov VB, Yushkov KB, Linde BB. Improvement in performance of a Teo2 acousto-optic imaging spectrometer. *J Opt A: Pure Appl Opt* (2007) 9(4):341–7. doi:10.1088/1464-4258/9/4/006

14. Harris SE, Wallace RW. Acousto-optic tunable filter. *J Opt Soc Am* (1969) 59(6):744–7. doi:10.1364/JOSA.59.000744

15. Y Chu, L Chen, H Wang, C ZHang, W Liu, P Wang, et al. editors. Research on edge enhancement of optical image based on acousto-optic filtering. In: Twelfth International Conference on Information Optics and Photonics, Xi'an, China, July 23–27, 2021 (Xi'an, China: SPIE) (2021).

16. Machikhin A, Gorevoy A, Batshev V, Pozhar V. Modes of wide-aperture acousto-optic diffraction in a uniaxial birefringent crystal. *J Opt* (2021) 23(12):125607. doi:10.1088/2040-8986/ac3368

17. R Abdlaty, S Sahli, J Hayward, Q Fang, editors. Hyperspectral imaging: Comparison of acousto-optic and liquid crystal tunable filters. In: *Medical ImagingPhysics of medical imaging*. Houston, TX: International Society for Optics and Photonics (2018).

18. A Beliaeva, G Romanova, editors. Energy efficiency of lighting systems based on acousto-optic filtration. *J Phys Conf Ser* (2021).

19. Lingying C, Qiang Z, Yuehong Q. Design of optical system for broadband and integrated aotf imaging spectrometer. *Acta Optica Sinica* (2021) 41(7):0722002. doi:10.3788/aos202141.0722002

20. J Zhu, L Li, X Guo, W Zhu, N An, editors. A multi-field of view hyperspectral imaging system based on mid-wave infrared. In: *4th optics young scientist summit (OYSS 2020)*. Ningbo, China: International Society for Optics and Photonics (2021).

21. Beliaeva AS, Romanova GE. Batshev VI, zhukova TIComputer modelling of acousto-optical diffraction in optical systems design. In: AM Zhurkin, editor. *Optical design and testing X*. Online Only, China: International Society for Optics and Photonics (2020).

22. Chen Y, Li W, Hyyppä J, Wang N, Jiang C, Meng F, et al. A 10-nm spectral resolution hyperspectral lidar system based on an acousto-optic tunable filter. *Sensors* (2019) 19(7):1620. doi:10.3390/s19071620

23. Kulak GV, Ropot PI, Bestugin AR, Shakin OV. Acousto-optical spectrum analyzer based on bessel light beams. *Problemy Fiziki, Matematiki i Tekhniki (Problems Phys Maths Technics)* (2021)(1) 19–23.

24. L Tv KKS, Kruglov SK. Application of the flicker noise filtering algorithm by changing the modulation frequency in an acousto-optic spectrum analyzer. *IOP Conf Ser : Mater Sci Eng* (2021) 1047(1):012113. doi:10.1088/1757-899X/1047/1/012113

25. Machikhin A, Batshev V, Pozhar V, Naumov A, Gorevoy A. Acousto-optic tunable spectral filtration of stereoscopic images. *Opt Lett* (2018) 43(5):1087–90. doi:10.1364/ol.43.001087

26. V Pozhar, M Bulatov, A Machikhin, V Shakhnov, editors. Technical implementation of acousto-optical instruments: Basic types. In: Journal of Physics: Conference series. Moscow, Russian Federation: IOP Publishing (2019).

27. Voloshinov VB, Porokhovnichenko DL, Dyakonov EA. Design of far-infrared acousto-optic tunable filter based on backward collinear interaction. *Ultrasonics* (2018) 88:207–12. doi:10.1016/j.ultras.2018.04.002

28. Batshev V, Machikhin A, Gorevoy A, Martynov G, Khokhlov D, Boritko S, et al. Spectral imaging experiments with various optical schemes based on the same aotf. *Materials* (2021) 14(11):2984. doi:10.3390/ma14112984

29. Mantsevich SN, Yushkov KB. Optimization of piezotransducer dimensions for quasicollinear paratellurite aotf. *Ultrasonics* (2021) 112:106335. doi:10.1016/j.ultras.2020.106335

30. Suhre DR, Denes LJ, Gupta N. Telecentric confocal optics for aberration correction of acousto-optic tunable filters. *Appl Opt* (2004) 43(6):1255–60. doi:10.1364/ao.43.001255

31. A Beliaeva, G Romanova, A Chertov, editors. Analysis of chromatic aberrations influence on operation of the tunable aotf-based source. *J Phys Conf Ser* (2021):2091/012012. doi:10.1088/1742-6596/2091/1/012012

32. KB Yushkov, VV Gurov, VY Molchanov, editors. Engineering of aotf transfer function for phase imaging microscopy and optical trapping. In: European Conference on Biomedical Optics. Munich Germany: Optical Society of America (2021).

33. V Batshev, S Boritko, A Kozlov, M Sharikova, V Lomonov, editors. Optical system of visible and short-wave infrared aotf-based spectral imaging device. In: *2021 wave electronics and its application in information and telecommunication systems*. St. Petersburg, Russia: WECONF IEEE (2021).

34. OD Moskaletz, MA Vaganov, VI Kazakov, AS Khomutov, editors. Measurement of optical spectrum by a spectral device based on an acousto-optic tunable filter with a stepwise tuning frequency. In: *2020 systems of signals generating and processing in the field of on board communications*. Moscow, Russia (2020).

35. Khokhlov DD, Machikhin A, Batshev V, Gorevoy A, Pozhar V. *Endoscopic spectral imagers based on acousto-optic filtration of light*. SPIE (2019).

36. Batshev V, Machikhin A, Martynov G, Pozhar V, Boritko S, Sharikova M, et al. Polarizer-free aotf-based swir hyperspectral imaging for biomedical applications. *Sensors* (2020) 20(16):4439. doi:10.3390/s20164439

37. GN Martynov, AV Gorevoy, AS Machikhin, VE Pozhar, editors. On inherent spatio-spectral image distortion in aotf-based imagers. In: *Optical measurement systems for industrial inspection XII*. Online Only, Germany: International Society for Optics and Photonics (2021).

38. Xu Z, Zhao H, Jia G, Sun S, Wang X. Optical schemes of super-angular aotf-based imagers and system response analysis. *Opt Commun* (2021) 498:127204. doi:10.1016/j.optcom.2021.127204

39. Lei S, Chunguang Z, Hao W, Jiangwei Y. Hyperspectral microimaging system based on double-filtering technology of acousto-optic tunable filter and its image analysis. *Laser Optoelectronics Prog* (2019) 55(3):032303.

40. L Denes, B Kaminsky, M Gottlieb, P Metes, editors. Factors affecting aotf image quality. In: Proceedings of the First Army Research Laboratory AOTF Workshop. Adelphi, Md: Army Research Laboratory (1997). Army Research Laboratory Report ARL-SR-54.

41. Pozhar VE, Machikhin AS, Gaponov MI, Shirokov SV, Mazur MM, Sheryshev AE. Hyper-spectrometer based on an acousto-optic tuneable filters for UAVS. *L&E* (2019) 27(3):99–104. doi:10.33383/2018-029

42. V Pustovoit, V Pozhar, M Mazur, V Shorin, I Kutuza, A Perchik, editors. *Double-aotf spectral imaging system*. Warsaw, Poland: Acousto-optics and PhotoacousticsSPIE (2005).

43. Zhang X, Zhang C, Chen Y, Wang H, Sheng Z, Huang X, et al. Study on the performance of double filtering based on an acousto-optic tunable filter. *Phys Scr* (2019) 94(11):115507. doi:10.1088/1402-4896/ab2061

44. V Batshev, A Machikhin, S Boritko, G Martynov, A Gorevoy, N Moiseeva, editors. Double-pass acousto-optic filtration for spectral imaging. In: 2021 International Conference on Information Technology and Nanotechnology, Samara, Russian Federation, September 20–24, 2021 (Samara, Russian Federation: ITNT IEEE) (2021).

45. Gupta N, Suhre DR. Effects of sidelobes on acousto-optic tunable filter imaging. *Opt Eng* (2017) 56(7):073106. doi:10.1117/1.oe.56.7.073106

46. Shi S, Lv X, Wang Z, Guo J, Huang Y. Ray tracing method for removing sidelobe laser interference in aotf-based hyperspectral imaging. *Appl Opt* (2021) 60(17):5186–94. doi:10.1364/ao.423016

47. Arellanes AO, Quintard V, Pérennou A. Spectral and temporal behavior of a quasi-collinear aotf in response to acoustic pulses: Simulations and experiments. *Appl Opt* (2022) 61(7):1687–94. doi:10.1364/ao.449028

48. SN Mantsevich, editor. Frequency locking effect in acousto-optic systems and its practical applications. In: *2019 wave electronics and its application in information and telecommunication systems (WECONF)*. St. Petersburg, Russia (2019).

49. Satorius DA, Dimmick TE, Burdge GL. Double-pass acoustooptic tunable bandpass filter with zero frequency shift and reduced polarization sensitivity. *IEEE Photon Technol Lett* (2002) 14(9):1324–6. doi:10.1109/lpt.2002.801111

50. A Machikhin, editor. Acousto-optical tunable filters: Applications in 3d imaging and multi-wavelength digital holography. In: *Digital holography and three-dimensional imaging*. Washington, D.C: Optical Society of America (2021).

51. Champagne J, Kastelik J-C, Dupont S, Gazalet J. Study of the spectral bandwidth of a double-pass acousto-optic system [Invited]. *Appl Opt* (2018) 57(10):C49–C55. doi:10.1364/ao.57.000c49

52. D Khoptyar, AA Subash, M Saleem, S Andersson-Engels editors. Wide-bandwidth diffused optical spectroscopy for pharmaceutical characterization. In: 2012 Asia Communications and Photonics Conference, Guangzhou, China, November 7-10, 2012 (Guangzhou, China: ACP IEEE) (2012).

53. D Khoptyar, A Subash, M Saleem, OHA Nielsen, S Andersson-Engels editors. Wide-bandwidth photon time of flight spectroscopy for biomedical and pharmaceutical applications. In: 2013-16th International Conference on Near Infrared Spectroscopy, La Grande-Motte, France, June 2–7, 2017 (La Grande-Motte, France) (2013).

54. R Abdlaty Q Fang, editors. *Acousto-optic tunable filter-based hyperspectral imaging system characterization*. San Francisco, CA: Design and Quality for Biomedical Technologies XIISPIE (2019).

55. Machikhin A, Batshev V, Pozhar V, Naumov A. Single-volume dual-channel acousto-optical tunable filter. *Opt Express* (2020) 28(2):1150–7. doi:10.1364/OE.383960

56. A Naumov, editor. Optical system of 3d aotf-based microscopic imager. *J Phys Conf Ser* (2021):2127/012038. doi:10.1088/1742-6596/2107/1/012038

57. Mazur M, Mazur L, Suddenok YA, Shorin V. Increase of an output optical signal of an acousto-optic monochromator upon frequency modulation of a control signal. *Opt Spectrosc* (2018) 125(4):594–8. doi:10.1134/s0030400x18100156

58. KV Zaichenko BS Gurevich, editors. Spectral selection using acousto-optic tunable filters for the skin lesions diagnostics. In: *European conference on biomedical optics*. Munich Germany: Optical Society of America (2021).

59. KV Zaichenko BS Gurevich, editors. Biochemical analyzer for medical diagnostics based on spectrophotometric principle and programmable light source. In: *European conference on biomedical optics*. Munich Germany: Optical Society of America (2021).

60. Zaichenko K, Gurevich B. *Features of electroencephalographic signals acousto-optic processing*. Online Only, France: SPIE (2020).

61. K Zaichenko B Gurevich, editors. Acousto-optic devices application for bioelectric signals wavelet processing. In: *2021 ural symposium on biomedical engineering*. Radioelectronics and Information Technology USBEREIT (2021).

62. Machikhin A, Pozhar V, Batshev V. An acousto-optic endoscopic imaging spectrometer. *Instrum Exp Tech* (2013) 56(4):477–81. doi:10.1134/s0020441213030202

63. Zaichenko K, Gurevich B. *Choice of photodetector characteristics for acousto-optic devices for bioelectric signals processing*. SPIE (2020).

64. Yushkov KB, Champagne J, Kastelik J-C, Makarov OY, Molchanov VY. Aotf-based hyperspectral imaging phase microscopy. *Biomed Opt Express* (2020) 11(12): 7053–61. doi:10.1364/boe.406155

65. He Z, Li C, Xu R, Lv G, Yuan L, Wang J. Spectrometers based on acousto-optic tunable filters for *in-situ* lunar surface measurement. *J Appl Remote Sensing* (2019) 13(2):027502.

66. Gorevoy A, Machikhin A, Martynov G, Pozhar V. Computational technique for field-of-view expansion in aotf-based imagers. *Opt Lett* (2022) 47(3):585–8. doi:10.1364/ol.438374

67. Vanhamel J, Dekemper E, Berkenbosch S, Clairquin R. Novel acousto-optical tunable filter (aotf) based spectropolarimeter for the characterization of auroral emission. *Instrumentation Sci Technol* (2021) 49(3):245–57. doi:10.1080/10739149.2020.1814809

68. Sierra JAR, Contreras GS, Rivera EKA, Isaza C, de Paz JPZ. A novel methodology to study particulate material/aerosol pollution via real-time hyperspectral acousto-optic intelligent spectrometry. In: *Health and well-being considerations in the design of indoor environments*. Hershey, Pennsylvania: Hershey, Pennsylvania: IGI Global (2021). 32

69. Korablev OI, Belyaev DA, Dobrolenskiy YS, Trokhimovskiy AY, Kalinnikov YK. Acousto-optic tunable filter spectrometers in space missions [Invited]. *Appl Opt* (2018) 57(10):C103–C19. doi:10.1364/ao.57.00c103

70. Seo Y, Park B, Yoon S-C, Lawrence KC, Gamble GR. Morphological image analysis for foodborne bacteria classification. *Trans ASABE* (2018) 61(1):5–13. doi:10.13031/trans.11800

71. Duocastella M, Surdo S, Zunino A, Diaspro A, Saggau P. Acousto-optic systems for advanced microscopy. *J Phys Photon* (2020) 3(1):012004. doi:10.1088/2515-7647/abc23c

72. AS Khomutov, VI Kazakov, OD Moskaletz, editors. Spectrometer based on acousto-optic tunable filter for contactless spectral monitoring in extreme conditions. In: *Wave electronics and its application in information and telecommunication systems (WECONF)*. St. Petersburg, Russia: (2020).

73. Bonah E, Huang X, Aheto JH, Osae R. Application of hyperspectral imaging as a nondestructive technique for foodborne pathogen detection and characterization. *Foodborne Pathog Dis* (2019) 16(10):712–22. doi:10.1089/fpd.2018.2617

74. Park B, Eady M, Oakley B, Yoon S-C, Lawrence K, Gamble G. Hyperspectral microscope imaging methods for multiplex detection of Campylobacter. *J Spectr Imaging* (2019) 8. doi:10.1255/jsi.2019.a6

75. Kang R, Park B, Ouyang Q, Ren N. Rapid identification of foodborne bacteria with hyperspectral microscopic imaging and artificial intelligence classification algorithms. *Food Control* (2021) 130:108379. doi:10.1016/j.foodcont.2021.108379

76. Erna KH, Rovina K, Mantihal S. Current detection techniques for monitoring the freshness of meat-based products: A review. *J Packag Technol Res* (2021) 5(3): 127–41. doi:10.1007/s41783-021-00120-5

77. Polschikova O, Machikhin A, Ramazanova A, Bratchenko I, Pozhar V, Danilycheva I, et al. An acousto-optic hyperspectral unit for histological study of microscopic objects. *Opt Spectrosc* (2018) 125(6):1074–80. doi:10.1134/s0030400x19020188

78. Baek I, Lee H, Cho B-k, Mo C, Chan DE, Kim MS. Shortwave infrared hyperspectral imaging system coupled with multivariable method for tvb-N measurement in pork. *Food Control* (2021) 124:107854. doi:10.1016/j.foodcont.2020.107854

79. L Chen, Y Chu, C Zhang, H Wang, S Fan, B Yan. editors. Hyperspectral imaging system based on fiber endoscope. In: Twelfth International Conference on Information Optics and Photonics, Xi'an, China, July 23-27, 2021 (SPIE) (2021).

80. Liu H, Yu T, Hu B, Hou X, Zhang Z, Liu X, et al. Uav-borne hyperspectral imaging remote sensing system based on acousto-optic tunable filter for water quality monitoring. *Remote Sensing* (2021) 13(20):4069. doi:10.3390/rs13204069

81. Ji Z, He Z, Gui Y, Li J, Tan Y, Wu B, et al. Research and application validation of a feature wavelength selection method based on acousto-optic tunable filter (aotf) and automatic machine learning (automl). *Materials* (2022) 15(8):2826. doi:10.3390/ma15082826